Iranian Journal of Veterinary Science and Technology

Received: 2025- Jul-13
Accepted after revision: 2025- Nov-29
Published online: 2025- Dec-01

RESEARCH ARTICLE

DOI: 110.22067/ijvst.2025.93330.1533

Cryo-infarction: a method of choice for the establishment of a rat model of myocardial infarction

Alireza Karimi[a], Maryam M. Matin[a,b], Azadeh Haghighitalab[a,c], Hossein Kazemi Mehrjerdi[d], Masoud Rajabioun[d], Mehrdad Aghasizadeh[a], Ahmad Reza Bahrami[a,b]

[a] Department of Biology, Faculty of Science, Ferdowsi University of Mashhad, Mashhad, Iran.
[b] Institute of Biotechnology, Ferdowsi University of Mashhad, Mashhad, Iran.
[c] Stem Cells and Regenerative Medicine Department, Academic Center for Education, Culture, and Research (ACECR) - Khorasan Razavi, Iran.
[d] Department of Clinical Sciences, Faculty of Veterinary Medicine, Ferdowsi University of Mashhad, Mashhad, Iran.

ABSTRACT

Ligation of the left anterior descending (LAD) coronary artery is a widely used method for inducing myocardial infarction (MI) in experimental models; however, it is associated with substantial limitations, including high mortality rates, excessive bleeding and variability in infarct size. Cryo-infarction has emerged as a promising alternative that may overcome these challenges by providing improved survival and reproducibility. In the present study, we aimed to refine the cryo-infarction method as a reliable and practical rat model for MI. Adult male Wistar rats underwent open-chest surgery under mechanical ventilation, followed by either LAD ligation or cryo-induced infarction. Model validation was performed using TTC (2,3,5-triphenyltetrazolium chloride) staining and immunofluorescence analysis, serum troponin I measurement, and electrocardiography assessment. Infarct severity was further evaluated by echocardiography, hematoxylin, and eosin staining, and Masson's trichrome staining. Our findings demonstrate that cryo-infarction provides several advantages over conventional ligation, including simplicity, reproducibility, and reduced mortality. These results highlight the potential of cryo-infarction as a standard approach for developing robust animal models, benefiting both basic and translational cardiovascular research.

Keywords

Heart, Myocardial infarction, Cryo-infarction, LAD, Rat model

Number of Figures: 9
Number of Tables: 1
Number of References:: 33
Number of Pages: 14

Abbreviations

AAR: Area at risk

AS: Atherosclerosis

Corresponding author: Ahmad Reza Bahrami
Email: ar-bahrami@um.ac.ir
Tel: +98(51)3880-5505

Introduction

Myocardial infarction, commonly referred to as a heart attack, is acute ischemia condition that results in irreversible damage to cardiac muscle tissue. This is commonly caused by blood clots that obstruct a coronary artery [1][2]. The clot formation or thrombosis that triggers myocardial infarction may arise from disrupted endothelial function, platelet activation, or coagulation factor imbalances, among other factors. The resulting ischemic injury to cardiomyocytes leads to cardiac dysfunction and potential complications such as arrhythmias, heart failure, or sudden cardiac death [3][4]. Researchers often seek to replicate myocardial infarction in laboratory animals to study its causes and explore therapeutic interventions. To study the process of the disease in detail, animal models have played a very important role in laboratory investigations for many decades [5]. Among available laboratory species, rats are widely used due to their cost-effectiveness, ease of handling, and genetic similarities to humans. These animals have helped researchers to create MI models and develop many novel therapeutic methods [6]. A variety of approaches have been developed to induce MI model and the success rate of the investigators depends on each method. The common procedures for the MI induction include: permanent ligation (PL), chemical methods (isoproterenol-induced MI model), and cryoinjury. Additionally, the high-fat diet method is used to study the pathology of coronary artery diseases (CADs) in animals. This approach involves feeding experimental animals with cholesterol-rich foods for a relatively long time, inducing hyperlipidemia, atherosclerosis (AS), and sclerotic plaques, resulting in stenosis in blood vessels and myocardial ischemia. Although animal models created with a high-fat diet closely mimic the natural progression of human CAD patients, this approach is labor-intensive and presents challenges in precisely controlling myocardial ischemia [6]. Rats are frequently selected for CAD studies because they are easy to maintain, have high survival rates, and are inexpensive to keep. However, the absence of a gallbladder and a natural resistance to spontaneous anti-AS formation limit their suitability as ideal CAD models. This character makes it difficult to induce AS lesions by a high-fat diet alone. Therefore, most researchers prefer to use a combination of drugs and/or injury to form AS lesions. Although the morphology of AS lesions and plaque rupture positions in rats are similar to those in humans, the underlying pathogenesis still differs from that observed in human CAD [6][7]. Pharmacological induction is relatively simple and usually uses abdominal, caudal, or sublingual vein injection of pituitrin or isoproterenol (ISO), which can result in short-term MI. The isoproterenol-induced acute myocardial infarction (AMI) model is a widely used and well-established non-surgical approach in rats. ISO is a chemical compound that produces extensive necrosis in the ventricular subendocardial region and interventricular septum. This model offers several advantages over surgical models, including low mortality rate, technical simplicity, and absence of post-surgical infections. Rats are commonly preferred for this model, but several other species, like mice and rabbits, are also reported to be used. The ISO-induced MI model is widely used in assessing the cardio-protective activity of natural as well as synthetic compounds [6][8]. However, this model is unsuitable for investigating autolysis recanalization in clinical settings. In the PL technique, an anesthetized rat undergoes left thoracotomy followed by LAD occlusion. This method requires surgical left thoracotomy in anesthetized rats, where the LAD is ligated [9][10]. LAD ligation induces complete ischemia, leading to irreversible oxygen deprivation, significant Area at risk (AAR) infarction, and permanent scar formation. This scar tissue is susceptible to pathological remodeling, ultimately contributing to the progression of heart failure. Furthermore, the anatomical site of coronary occlusion significantly influences the infarction extent, with proximal ligations producing larger infarcts than distal occlusions; occlusion closer to the heart's base results in a larger and more severe injury. The PL technique typically produces extensive myocardial damage, with infarcts generally encompassing 30-40% of the total myocardial area [6][11]. A major advantage of employing the PL method is that it results in a substantial infarction, leading to clearer distinctions in cardiac function between sham-operated and MI animals [12]. The surgical ligation model is a widely used method for inducing AMI by ligating different regions of the coronary artery, with the LAD coronary artery ligation being the most common. This method was first introduced by Johns and Olson in 1954 and has since been adapted for use in both small and large animal species. Mice and rats are commonly employed

Abbreviations-Cont'd

CAD: Coronary artery disease
EF: Ejection fraction
ECG: Electrocardiography
FS: Fractional shortening
ISO: Isoproterenol
LAD: Left anterior descending
LDL: Low-density lipoprotein
LV: Left ventricle
MI: Myocardial infarction
PL: Permanent ligation
ROS: Reactive oxygen species
TBS: Tris-buffered saline

in laboratory settings for surgical ligation due to their numerous benefits compared to larger animals. The main limitations of LAD model are high mortality rate, post-surgical infection, variation in infarct size from 4-59%, requirement of expert hands, and an artificial ventilator. Performing this technique on mice is challenging and necessitates advanced surgical proficiency with microsurgical techniques. Complications can arise due to tissue damage, high perioperative mortality rates, intraoperative bleeding, lung damage or collapse, ligation errors, or inadequate ventilation. Cryoinjury represents an alternative method for inducing permanent myocardial injury. In this model, a pre-cooled rod at -196°C is applied to the heart, for multiple times, to cause injury. Cryoinjury leads to progressive structural reorganization and volumetric expansion of the left ventricular chamber [12]. The cryoinjury technique models myocardial infarction through controlled focal freezing of cardiac tissue. The cryo-infarction technique has been explored as a viable method for inducing MI in experimental models. The cryoinjury model produces well-defined myocardial damage characterized by histological features typical of infarction, including coagulation necrosis, hemorrhagic regions, inflammatory responses, and subsequent tissue repair with scar formation. This pathological progression ultimately results in heart failure, closely mimicking the outcomes observed in LAD ligation models, while providing a valuable alternative for investigating cardiac injury. Compared to surgical occlusion techniques, the cryodamage approach demonstrates superior technical simplicity and experimental reproducibility, as it eliminates the need for intricate vascular interventions [4]. In the present study, we propose that cryoinjury provides an optimal balance between reproducibility and physiological relevance for modeling MI and associated immune responses in rats. To our knowledge, no previous study has systematically compared cryoinjury with established MI induction methods.

Results

Cryo-induced myocardial infarction produces localized necrosis comparable to LAD ligation

The cryo method successfully induced myocardial infarction in rats. Post-procedure, a bright white and sunken region was observed at the site of cryo-injury, confirming the induction of localized infarction. Notably, this color change closely resembled the pale necrotic regions typically observed in LAD-ligation models, indicating a comparable loss of tissue viability. Quantitative analysis using TTC-stained sections revealed an infarct size of 12.52% in cryo-MI hearts (Figure 1A, B).

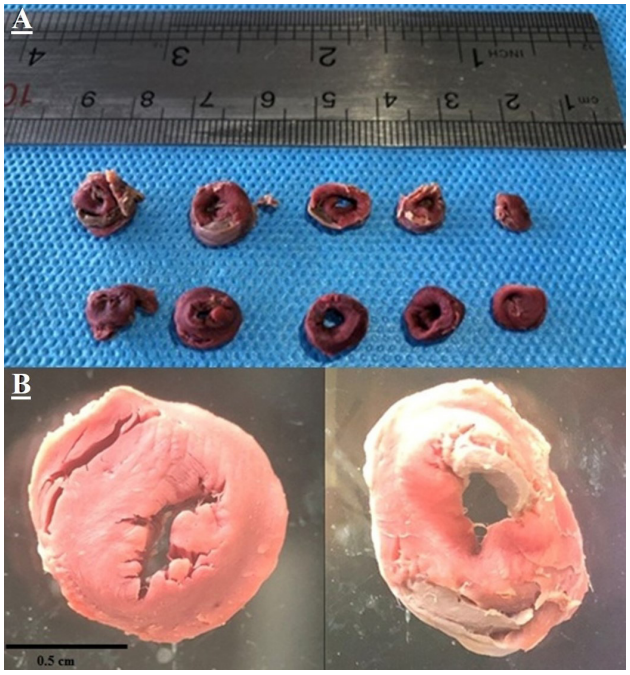

Figure 1.
Cryo-induced myocardial infarction shows pale necrotic regions compared to uniform red tissue in sham hearts. (A) The top row shows cryo-induced myocardial infarction, characterized by pale regions indicating infarcted tissue, while the bottom row represents the sham group with uniformly red myocardium, consistent with viable tissue. (B) Higher magnification of representative TTC-stained heart sections from sham (left) and cryo-MI (right) groups, 24 h post-surgery. The infarcted area in the cryo-MI sample was quantified as 12.52% using ImageJ software. Scale bar = 0.5 cm.

Cryo-induced myocardial infarction is associated with increased apoptosis and macrophage infiltration compared to sham

Immunofluorescence analysis revealed an increased accumulation of caspase-3 positive cells and expression of the macrophage marker CD68, in cryo-MI hearts compared to sham operated controls, indicating enhanced apoptosis and macrophage infiltration (Figures 2, 3). Quantitative analysis confirmed significant differences between groups ($p < 0.001$ for caspase-3; and $p < 0.01$ for CD68).

Cryo-induced myocardial infarction exhibits higher early survival than LAD ligation

Qualitative troponin testing was positive in all animals subjected to cryo-MI and LAD-MI procedures, whereas sham operated rats consistently tested negative. Survival analysis revealed a marked difference in early mortality between the two surgical approaches. Within the first 24 h post-surgery, 28 of 95 rats in the cryo-MI group died, corresponding to a survival rate of 70.59%. In contrast, 64 out of 102 rats in the LAD-

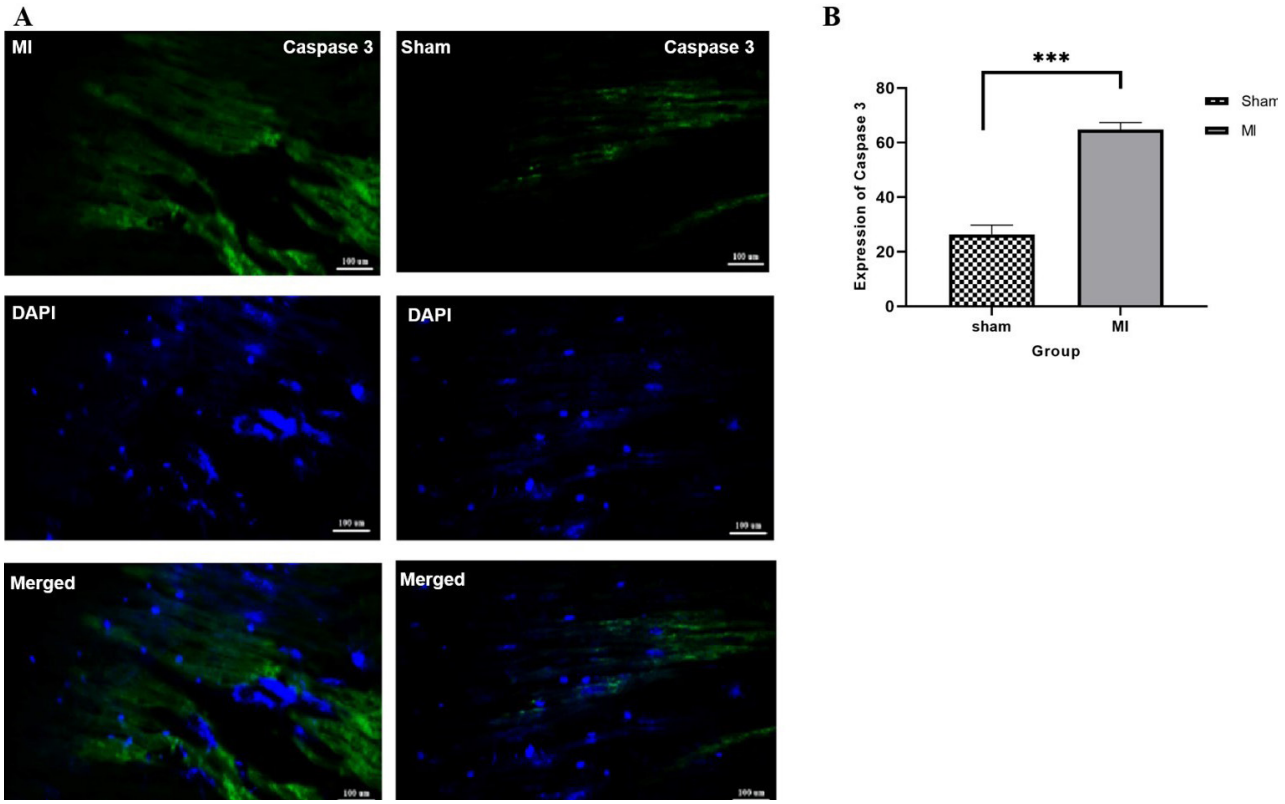

Figure 2.
Immunofluorescence detection and quantification of caspase-3 positive cells in sham and cryo-MI hearts. (A) Immunofluorescence staining of caspase 3 positive cells in sham and cryo-MI groups. Caspase-3 positive cells appear green, and nuclei are counterstained with DAPI (blue). Merged images show colocalization. Scale bar represents 100 µm. (B) Quantification was expressed as the percentage of caspase-3 positive cells relative to total nuclei. Quantitative analysis reveals a significant increase in caspase-3 expression in the cryo-MI group compared to sham ($p < 0.001$) (48 h after MI).

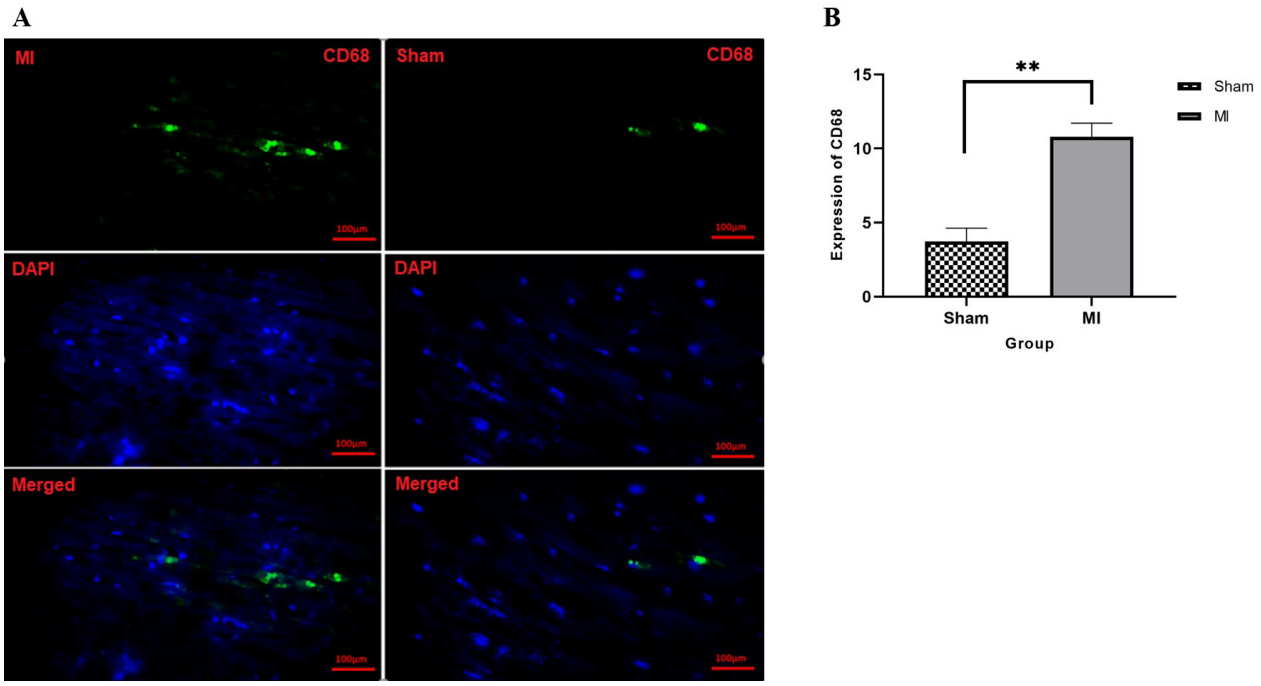

Figure 3.
Increased CD68⁺ macrophage infiltration in cryo-induced myocardial infarction compared to sham controls. (A) Immunofluorescence staining of CD68⁺ macrophages in sham and cryo-MI groups. CD68⁺ cells are shown in green, and nuclei are counterstained with DAPI (blue). Merged images illustrate macrophage localization within cardiac tissue. (B) Quantification was expressed as the percentage of CD68⁺ cells relative to total nuclei. Bar graph showing a significant increase in CD68⁺ macrophage infiltration in the cryo-MI group compared to sham controls ($p < 0.01$) (48 h after MI). Scale bar represents 100 µm.

MI group died during the same period, resulting in a substantially lower survival rate of 38.76% (Table 1), indicating higher early mortality in LAD-MI.

Cryo- and LAD-induced myocardial infarction cause ST-segment elevation and rhythm alterations

ECG recordings demonstrated pronounced ST-segment elevation in both cryo-MI and LAD-MI groups compared with sham controls (Figure 4). LAD-MI produced severe rhythm disturbances and high-amplitude changes, whereas cryo-MI exhibited abnormal but less pronounced alterations, consistent with localized myocardial damage.

Table 1.
Survival ration of surgical procedures.

Type of surgery	Total number of rats	Number of surviving rats 24 h after surgery	Survival percentage of rats 24 h after surgery
Cryo	95	67	70.52
LAD	102	38	38.76

Cryo- and LAD-induced myocardial infarction cause persistent decline in cardiac function

Serial echocardiography demonstrated significant reductions in fractional shortening (FS) and ejection fraction (EF) in both cryo-MI and LAD-MI groups compared with sham controls (Figure 5 A, B). Both MI models exhibited a sharp decline in FS and EF as early as day 1 post-surgery, followed by partial functional recovery by day 28 and persistent dysfunction through day 55. In contrast, sham-operated animals maintained stable FS and EF values throughout the study, indicating that cryo- and LAD-induced infarction result in sustained impairment of cardiac contractility.

Cryo-induced MI causes greater fibrotic remodeling than LAD ligation

Histological analysis revealed normal myocardial architecture, characterized by intact cardiomyocytes and preserved tissue organization in sham hearts (Figure 6I, 6II). In contrast, LAD-MI hearts at day 7 post-infarction, exhibited severe pathological alterations, including interstitial edema, mixed inflammatory infiltrates within the pericardium, cardiomyocyte

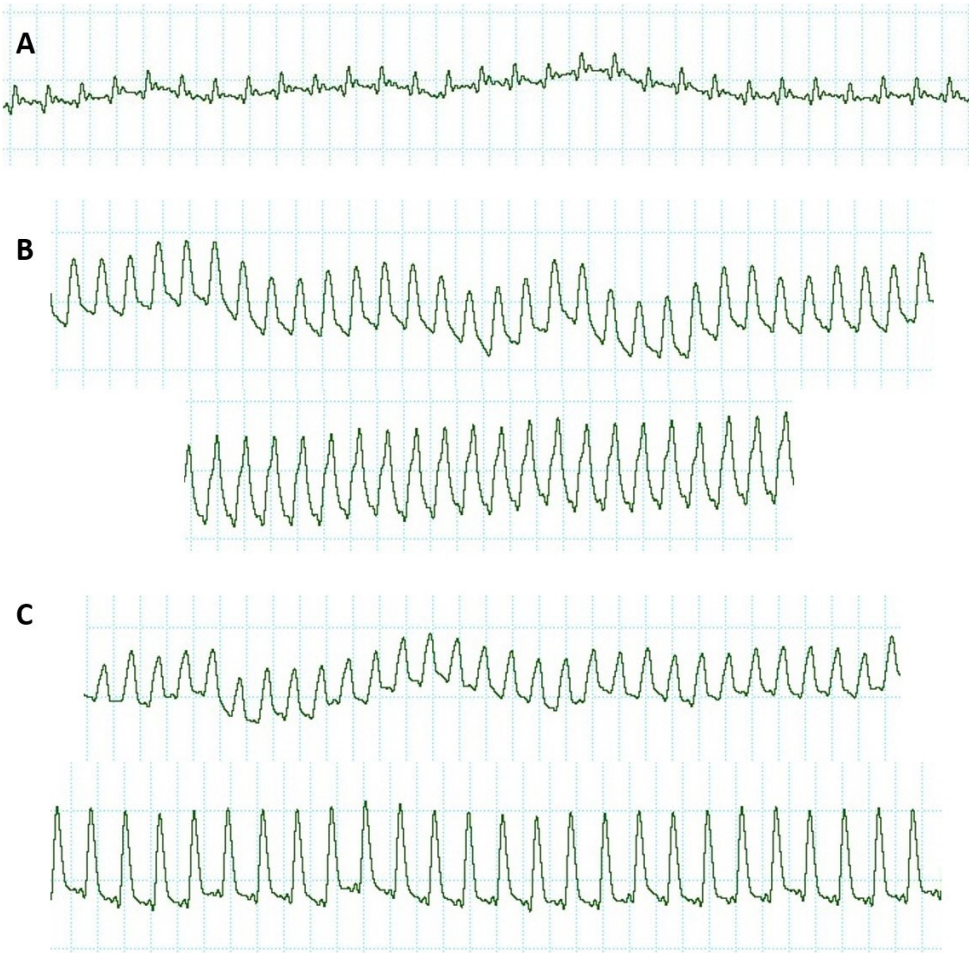

Figure 4.
Representative ECG waveforms in sham and MI models of myocardial infarction.
(A) Normal ECG pattern from sham-operated rats. (B) ECG waveform following LAD-induced myocardial infarctionin two rats, showing marked alterations in rhythm and amplitude. (C) ECG waveform following cryo-induced myocardial infarction in two rats, demonstrating distinct changes compared to sham controls. Compared to sham, LAD ligation produces severe rhythm disturbances and high-amplitude changes, while cryo-induced MI shows abnormal but less pronounced alterations, reflecting localized rather than extensive damage.

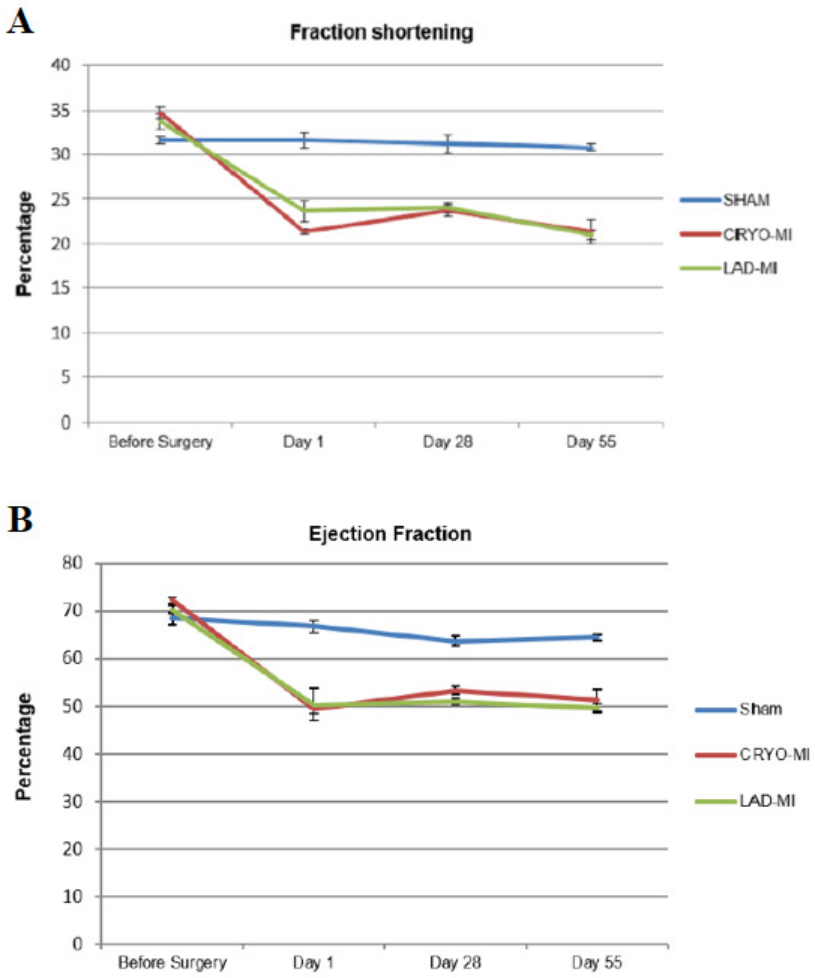

Figure 5.
Longitudinal decline in fractional shortening and ejection fraction after myocardial infarction. (A) FS was measured at baseline (pre-surgery), day 1, day 28, and day 55 post-procedure in sham (n = 5), LAD-MI (n = 3), and cryo-MI (n = 3) groups. Both LAD-MI and cryo-MI models exhibited a sharp reduction in FS by day 1, followed by partial recovery at day 28 and sustained impairment through day 55, whereas sham animals maintained stable FS values throughout. (B) EF was measured at baseline (pre-surgery), day 1, day 28, and day 55 post-procedure in sham (n = 4), LAD-MI (n = 3), and cryo-MI (n = 3) groups. Both LAD-MI and cryo-MI models exhibited a sharp reduction in EF by day 1, followed by minimal recovery at day 28 and persistent dysfunction through day 55, whereas sham animals maintained near-normal EF values throughout.

degeneration and necrosis, and hemorrhagic necrosis localized to the infarct border zone (Figure 6IIIA–F). In comparison, cryo-MI hearts at the same time point displayed focal necrosis accompanied by mixed inflammatory cell infiltration, interstitial edema, and eosinophilic changes confined to the cryo-injured region (Figure 6IVA-D). By day 55, chronic remodeling was evident in both models. LAD-MI hearts demonstrated granulation tissue formation, fibroblast proliferation, and early collagen deposition, along with pericardial thickening and fibrosis (Figure 7A-E). In contrast, cryo-MI hearts developed large, pale, homogeneous regions composed of acellular, densely collagenous scar tissue replacing functional myocardium, with adjacent hypertrophied cardiomyocytes indicative of compensatory remodeling (Figure 8). Masson's trichrome staining at day 56 confirmed extensive fibrotic replacement and pronounced ventricular wall thinning in cryo-MI hearts, whereas LAD-MI hearts exhibited localized collagen deposition restricted to the infarct zone, with relative preservation of overall chamber geometry (Figure 9). Quantitative analysis demonstrated significantly greater collagen deposition in cryo-MI hearts (10.99%) compared to LAD-MI hearts (6.19%), highlighting the more pronounced fibrotic remodeling associated with cryo-induced infarction.

Discussion

This study aimed to further investigate the cryo-infarction technique as a reliable approach for establishing a MI model in rats and to compare its outcomes with those obtained using the LAD coronary artery ligation method. Cryoinjury and LAD ligation are among the most commonly employed techniques for inducing MI in rodent models. Cryoinjury relies on the controlled application of subzero temperatures using a cryoprobe, resulting in localized necrosis through ice crystal formation and cellular disruption. A key advantage of this approach is the ability to precisely target specific myocardial regions and generate highly reproducible infarcts by adjusting probe temperature and contact duration. In contrast, LAD ligation induces MI through occlusion of the left anterior descending coronary artery, a major vessel supplying oxygenated blood to the myocardium, thereby producing ischemia that leads to extensive infarction, and closely resembles clinical coronary occlusion [13][14].

Figure 6.
Histopathological changes in sham, LAD-MI, and cryo-MI hearts. (I, II) Sham group shows normal myocardial architecture with intact cardiomyocytes and preserved tissue organization (400×, scale bar represents 50 µm). III (A-F) LAD-MI hearts at day 7 exhibit severe pathological changes, including interstitial edema, pericardial mixed inflammatory infiltrates, cardiomyocyte degeneration and necrosis, hemorrhagic necrosis, and co-localization of necrosis with inflammation and edema (100×, scale bar represents 200 µm–400×, scale bar represents 50 µm). (A) Interstitial edema with widened intramuscular spaces (arrow; H&E, 400×, scale bar represents 50 µm). (B) Pericardial mixed inflammatory infiltrate (arrows; H&E, 100×, scale bar represents 200 µm). (C, D) Cardiomyocyte degeneration and necrosis with mononuclear cell infiltration (arrows; H&E, 400×, scale bar represents 50 µm). (E) Co-localization of myocyte necrosis (black arrow), inflammatory infiltrate (blue arrow), and interstitial edema (stars; H&E, 400×, scale bar represents 50 µm). (F) Hemorrhagic necrosis showing degenerated cardiomyocytes (yellow arrow), hemorrhage (black arrow), inflammation (blue arrow), and edema (star; H&E, 400×). All images represent characteristic findings from the infarct border zone. IV (A-D) Cryo-MI hearts at day 7 display focal necrosis with mixed inflammatory cell infiltration, interstitial edema, and eosinophilic changes in the cryoinjured region (100×, scale bar represents 200 µm–400×, scale bar represents 50 µm). (A, B) Necrotic cardiomyocytes with mixed inflammatory infiltrate (mononuclear and polymorphonuclear leukocytes, arrows; H&E, 100×, scale bar represents 200 µm). (C) High-magnification view of necrotic myocardium with leukocyte infiltration (H&E, 400×, scale bar represents 50 µm). (D) Pericardial mixed inflammatory cell infiltration (H&E, 400×, scale bar represents 50 µm). All sections show characteristic interstitial edema and eosinophilic changes in the cryoinjured region.

Karimi et al., IJVST 2026; Vol.18, No.2
DOI: 10.22067/ijvst.2025.93330.1533

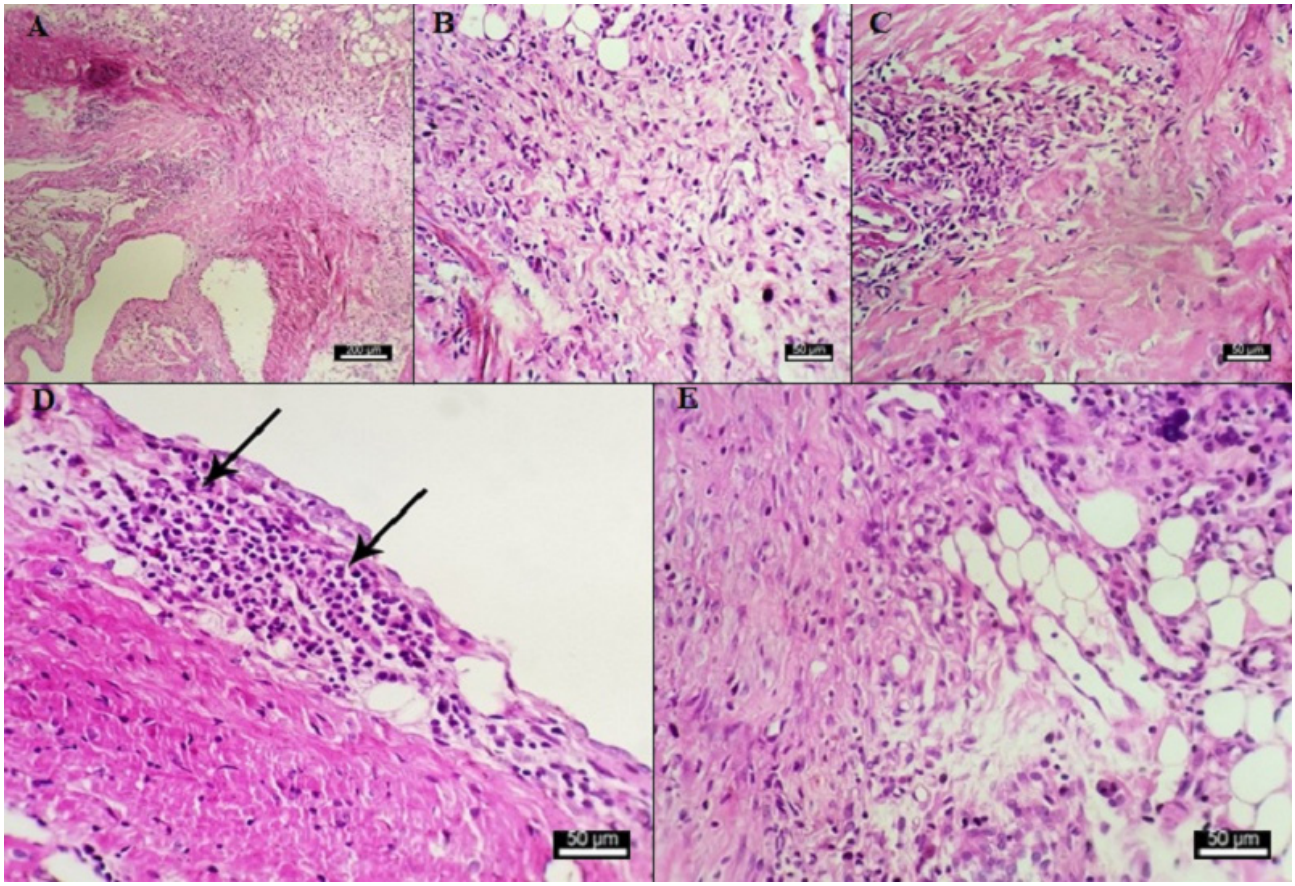

Figure 7.
Chronic histopathological changes in LAD-myocardial infarction at day 55.
(A–C) Cardiomyocyte necrosis with granulocyte and mononuclear cell infiltration, accompanied by granulation tissue formation, fibroblast proliferation, and early collagen deposition (100×- scale bar represents 200 µm, 400×-scale bar represents 50 µm). (D) Mixed inflammatory cell infiltration in the pericardium (arrows; 400×, scale bar represents 50 µm). (E) Thickened, fibrotic pericardium with dense inflammatory infiltrate (400×, scale bar represents 50 µm).

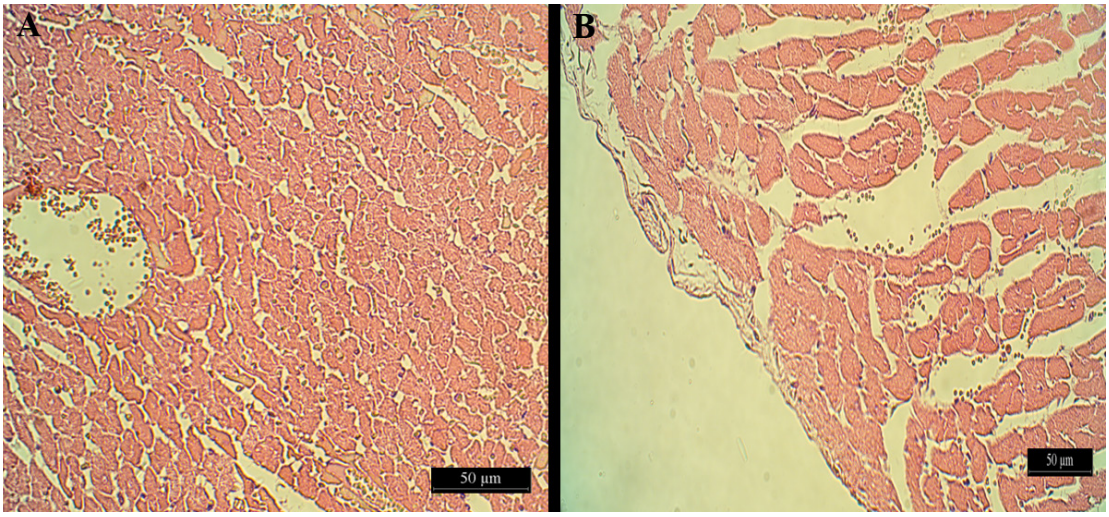

Figure 8.
Chronic structural remodeling in cryo-induced myocardial infarction at day 55. (A) Large, pale, homogeneous region representing an acellular, densely collagenous scar replacing functional myocardium. (B) Adjacent viable myocardium exhibiting hypertrophied cardiomyocytes, indicative of compensatory remodeling under increased hemodynamic load (400×, scale bar represents 50 µm).

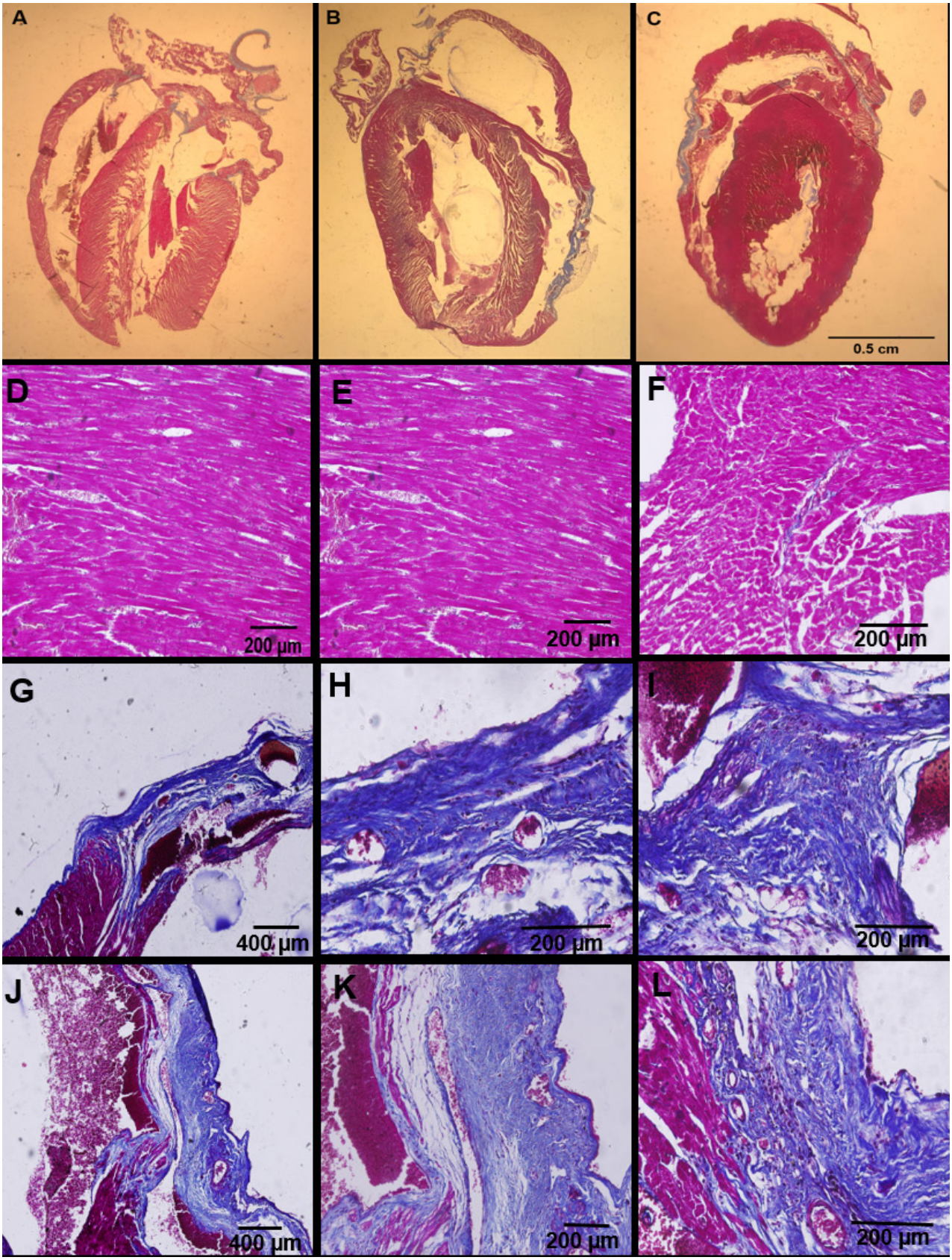

Figure 9.
Fibrotic remodeling at 56 days post-myocardial infarction, visualized using Masson's trichrome staining. (A) Sham group: No detectable collagen deposition (blue), indicating preserved myocardial architecture. (B) Cryo-MI group: Extensive fibrotic replacement (blue) accompanied by marked ventricular wall thinning. (C) LAD-MI group: Prominent collagen deposition (blue) localized to the infarct zone, consistent with scar formation. Cryo-MI hearts exhibit extensive, transmural fibrosis accompanied by pronounced ventricular wall thinning, whereas LAD-MI hearts show scar formation restricted to the infarct territory, preserving overall chamber geometry. Magnified view of each experimental group is provided in D-L. (D-F) Sham group: Normal myocardial architecture without detectable collagen deposition. (G-I) Cryo-MI group: Extensive, transmural fibrotic replacement (blue) accompanied by pronounced ventricular wall thinning. (J-L) LAD-MI group: Collagen deposition (blue) restricted to the infarct territory, preserving overall ven-

Each method presents distinct advantages and limitations. LAD ligation is well established and widely accepted, but it requires advanced microsurgical expertise, stereomicroscopic visualization, and precision instrumentation. Importantly, infarct size in the LAD model is highly operator dependent, ranging from 10–45% of the LV in inexperienced hands, while experienced operators achieve consistent infarcts (~35 ± 5%). Moreover, LAD ligation carries a high risk of procedural complications, including cardiac perforation and hemorrhage, contributing to elevated perioperative mortality. In the present study, early mortality was significantly higher in LAD-MI rats (70.59%) compared to cryo-MI rats (38.76%), underscoring the safety advantage of cryoinjury [15][12][16]. By comparison, cryoinjury offers superior control over infarct localization and size, thereby minimizing variability and reducing procedural complexity. Importantly, cryo-MI minimizes bleeding risk and allows reproducible induction of focal myocardial damage, making it particularly suitable for studies requiring localized injury. However, LAD ligation produces extensive infarctions and severe LV dilation, which may be advantageous for investigating advanced heart failure mechanisms. It is also important to recognize that rodent exhibit compensatory hypertrophy following MI, which often preserves ejection fraction despite large infarct sizes (>30% LV), a response that differs from human pathophysiology. This limitation should be considered when translating findings from rodent MI models to clinical settings [16][15][12]. In the present study, MI induction was confirmed by elevated troponin I levels, ECG abnormalities, and echocardiographic evidence of impaired cardiac function, consistent with Global MI Task Force criteria. Troponin I, a highly specific biomarker of myocardial injury, was positive in all cryo-MI and LAD-MI rats, validating successful infarction. Following myocardial damage, cTnI is released into the circulation within 4 to 6 h of injury, and its exceptional tissue specificity and diagnostic sensitivity has established it as the clinical gold-standard for MI diagnosis. The rapid troponin I assay employed in this study utilizes antibody coated particles and a marker reagent capable of detecting troponin I in whole blood or serum with a detection threshold of 1 ng/ml. In healthy rats, FS and EF typically range between 30-35% and 65-75%, respectively. However, the post-MI echocardiography analyses in the present study indicated that both cryo- and LAD-MI animals exhibited a marked reduction in FS (to 20-25%) and EF (to approximately 50%), with persistent dysfunction observed through day 55. Histological analysis demonstrated acute necrosis and inflammatory infiltration in both models, with cryo-MI hearts exhibiting focal injury and LAD-MI hearts showing extensive hemorrhagic necrosis. Chronic remodeling differed substantially as Masson's trichrome staining revealed greater collagen deposition and transmural fibrosis in cryo-MI hearts (10.99%) compared to LAD-MI hearts (6.19%), accompanied by ventricular wall thinning and hypertrophy of adjacent myocardium [8][17][18][19][20]. Immunofluorescence analysis further confirmed these observations, revealing increased caspase-3 expression and enhanced $CD68^{+}$ macrophage infiltration in cryo-MI hearts. These findings indicate robust apoptotic activity and inflammatory response. Our results suggest that cryoinjury induces localized but severe cellular stress, triggering apoptosis and immune cell recruitment. While such inflammatory responses may contribute to progressive fibrosis, they also provide a controlled microenvironment for studying post-MI remodeling processes and evaluating therapeutic interventions [21][22]. Overall, these data demonstrate that cryoinjury represents a reproducible, technically less demanding, and safer alternative to LAD ligation for inducing MI in rats, particularly when localized infarction and reduced mortality are desired. Conversely, LAD ligation remains the preferred approach for modeling large infarcts and advanced heart failure studies. Thus, selection of the appropriate MI model should be guided by experimental objectives, balancing infarct size, reproducibility, and translational relevance [12][17]. In summary, although cryoinjury and LAD ligation both result in comparable long-term LV dysfunction, cryoinjury offers distinct advantages. This method resulted in attenuated remodeling, formation of more compact and uniform scar tissue, and significantly higher survival rates compared to LAD ligation. Importantly, cryoinjury scars persist indefinitely, providing a stable and reproducible platform for investigating scar-region pathophysiology and long-term remodeling. Furthermore, cryoinjury consistently generates infarcts of uniform size and shape with precise spatial localization, making it an attractive model for preclinical studies focused on therapeutic interventions and mechanistic research [23][24][4][12].

Materials & Methods

Ethical approval

This study was conducted in accordance with ethical standards and received approval from the Ferdowsi University of Mashhad (FUM) Research Ethics Committee [Approval No: IR.UM.REC.1401.269].

Animal subjects

Adult male Wistar rats (250-300 g) were kept under standard conditions (23 ± 2°C; a 12-h light/dark cycle) with ad libitum access to standard food and water. The rats were bred and maintained in the animal house of FUM. All experimental procedures were conducted

in accordance with applicable guidelines and regulations, including the ARRIVE 2.0 guidelines. Fifteen male rats aged 60-90 days were randomly assigned into three groups: sham operated controls (group 1, n=5), LAD group (group 2, n=5), and Cryo group (group 3, n=5). During the experiments, the animals were randomly divided into three groups using Excel software (version 2016).

Prior to anesthesia, body weight and temperature were recorded for all animals. Anesthesia was induced via injection of ketamine (100 mg/kg; Alfasan 10%) and xylazine (10 mg/kg; Interchemie 2%) mixed in a 2:1 ratio. Additionally, meloxicam (1 mg/kg; RazakPharma 2%) was administered intramuscularly as a preemptive analgesic. Adequate depth of anesthesia was confirmed by the absence of the toe-pinch reflex and was monitored throughout the surgical procedure. Endotracheal intubation was performed by placing an angiocath (Vaccess I.V. Cannula green) in the trachea, with visualization aided by a flashlight in a darkened room. Mechanical ventilation was performed by connecting the endotracheal tube to the modified Babylog 8000 Drager ventilator (O_2 Vol=60, insp. Flow V=2 (l/min), Pinsp=30 (mbar), (TI=0.2 s). The aseptic condition was maintained during the survival surgery. Before surgery, ophthalmic ointment was applied to prevent corneal desiccation. After the surgery, animals were monitored for body temperature, heart rate, and signs of pain until full recovery. Rats were removed from ventilator and placed in individual cages with a heating pad positioned at one end to maintain normothermia. Water was made freely available. Sterile saline (0.5 ml) was administered subcutaneously following the surgery. Enrofloxacin (10 mg/kg) was administered immediately after the surgery and continued during recovery [4][25]. Antibiotic injections were given every 12 h and analgesics were administered every 24 h for 3 consecutive days following surgery [25][26].

Induction of myocardial infarction

Animals were left to reach steady breathing and their chests were opened at the fourth left intercostal space using surgical scissors. The space was opened without cutting muscle tissue to minimize bleeding. Then a chest retractor was placed to maintain exposure. The pericardium was opened but preserved whenever possible [25] [27]. The LAD was identified and tied using a 6-0 Prolene (polypropylene blue monofilament 209127) suture [28]. In the cryo-MI group, a cryoprobe consisting of a 3 mm diameter copper rod, was immersed in liquid nitrogen for two min. After exposure of the heart and opening of the pericardium, the cryo-infarction was induced by applying the cryoprobe tip to the anterior wall of the left ventricle for 10 seconds [4]. Sham control animals underwent the same surgical exposure without LAD ligation or cryo application. After completion of the procedure, the chest retractor was removed and the ribs were sutured using 4-0 Prolene (20 mm polyglycolate coated violet) suture. After closing the ribs, the ventilator output was briefly interrupted (1-2 seconds) to ensure proper breathing. The skin was closed using continuous 20 mm 4-0 Prolene sutures [28].

Infarct size measurement

Myocardial infarction size was assessed using 2,3,5-triphenyltetrazolium chloride (TTC) staining. Hearts were rapidly excised, flash-frozen at -80°C, and transversely sectioned into 2 mm-thick slices. Sections were incubated in 2% TTC solution at 37°C, for 30 min, followed by fixation in 10% neutral buffered formalin for 24 h. After rinsing with saline, the unstained infarcted regions were clearly demarcated from viable brick-red stained myocardium, enabling precise topographic documentation of ischemic damage [29][30].

Immuno-histochemistry analysis

Excised tissues were fixed in 10% neutral buffered formalin for 24–72 h, dehydrated through graded ethanol series (70%, 80%, 90%, 100%; 50 min each), cleared in xylene, and embedded in paraffin. Sections (5 µm thick) were prepared using a Leica RM2135 microtome and mounted on silanized slides. Antigen retrieval was performed by microwaving sections in 1× Tris-buffered saline (TBS; Sigma, T5912) until boiling, followed by incubation for 20 min in the heated solution. After three washes in phosphat buffer saline (PBS) (5 min each), sections were permeabilized with 0.3% Triton X-100 (Sigma, T8787) for 30 min and blocked with 10% goat serum (Sigma, G9023) for 45 min. Primary antibodies against caspase-3 (orb10237) and CD68 (orb388936) were applied at a dilution of 1:100 in PBS and incubated for 24 h at 2–8°C in a humidified chamber. Sections were washed four times (5 min each) and incubated with secondary antibodies (CD68: orb688924, caspase3: orb688925; 1:150 dilution) at 37°C for 1.5 h in the dark, then washed three times. DAPI (Sigma-D9542) was applied for 20 min, followed by PBS washing steps. Slides were mounted with glycerol and PBS and examined using a fluorescent microscope (Olympus).

Biochemical analysis of troponin in serum

Blood samples were collected 24 h post surgery from the retroorbital sinus and centrifuged at 3000 × *g* for 5 min at 4°C. Serum samples were immediately analyzed for troponin I using the Cardiac Troponin I Cassette Tape (Vitrotec CTN00-08), a rapid immunochromatographic assay for whole blood or serum. For analysis, 50 µl of serum was added to the sample, followed by 40 µl of cTnI buffer provided in the kit. A control line indicated proper test performance and sufficient sample volume.

Hematoxylin-Eosin staining

H&E staining was performed to assess cardiac morphology and confirm myocardial infarction. Heart tissues were collected at 7 and 55 days post-surgery, fixed in 10% formalin, sectioned at 5 µm, and stained with hematoxylin and eosin. Necrotic areas were examined using an Olympus BX-51 microscope equipped with a digital camera.

Electrocardiography and echocardiography

On day 7, rats underwent ECG recording under anesthesia (ketamine 75 mg/kg, xylazine 10 mg/kg) using the PowerLab Electrophysiological System (ML11, ADInstruments, Australia). Electrodes were placed on the right and left forelimbs. FS, and EF were assessed as indicators of left ventricular function. FS reflects the percentage reduction in ventricular diameter during systole, while EF represents the proportion of blood ejected from the left ventricle per heartbeat, calculated as:

EF="Stroke Volume" /"End-Diastolic Volume" ×100

Normal EF in rats ranges from 65–75%, with reductions indicating impaired cardiac performance [31]. Echocardiography (MyLab 30Gold VET, 8–10 MHz transducer) was performed after chest hair removal one day before surgery and on days 1, 28, and 55 post-surgery to monitor cardiac performance on anesthetized rats.

Masson's trichrome staining for collagen detection

Masson's trichrome staining was used to evaluate collagen deposition in cardiac tissue. In this method, collagen fibers appear blue, nuclei black, and cytoplasmic components red. Heart tissues were harvested 55 days post-surgery, fixed in 10% neutral buffered formalin for 24 h, and embedded in paraffin. Serial sections (5 µm) were prepared from regions of interest using a microtome. Images were captured using an OLYMPUS stereomicroscope (SZH-ILLK, Japan) [32][33].

Statistical analysis

Quantification of caspase-3 and CD68 expression was performed using ImageJ software. Statistical analyses were conducted using GraphPad Prism 10.3. Analyses included both sham and cryo-MI groups.

Authors' Contributions

AK: Investigation, Visualization, Software, Formal analysis, Data acquisition, Methodology, Writing - original draft preparation. MMM: Funding acquisition, Project administration, Supervision, Methodology, Validation, Resources. AH: Project administration, Supervision, Methodology, Investigation, Validation. HKM: Supervision, Methodology, Validation. MR: Supervision, Methodology, Data Acquisition, Visualization. MA: Methodology, Data acquisition, Visualization. ARB: Conceptualization, Funding acquisition, Project administration, Supervision, Methodology, Validation, Visualization, Resources. All authors were involved in writing, reviewing, and editing, and approved the final version.

Acknowledgements

We would like to express our sincere gratitude to the staff of the Mashhad Academic Jahad Medical Diagnostic Laboratory and the Veterinary Clinic, especially Mr. Barati, for their invaluable support. We also extend our special thanks to Mohammad-Hasan Mollaei, Dr. Hamidreza Kazerani and Navid Nateghi for their assistance and contributions throughout this study. We also extend our thanks to the laboratory technicians and postgraduate students in the Molcular Biology Laboratory of FUM for their assistance. This work was supported by Ferdowsi University of Mashhad)Grant No. 59386(and the National Institute for Medical Research Development (NIMAD, Grant No. 957797). The funding body had no role in study design, data collection and analysis, decision to publish, or preparation of the manuscript.

Conflict of interest

The authors declare that there is no conflict of interest.

References

1. Fathima SN. An update on myocardial infarction. Curr Res Trends Med Sci Technol. 2021;1:95.

2. Choo EH, Chang K, Lee KY, Lee D, Kim JG, Ahn Y, et al. Prognosis and predictors of mortality in patients suffering myocardial infarction with non-obstructive coronary arteries. J Am Heart Assoc. 2019;8(14):e011990. Doi:10.1161/JAHA.119.011990.

3. Mirzavi F, Ebrahimi S, Ghazvini K, Mehr SMH, Hashemy SI. Diagnostic, prognostic, and therapeutic potencies of circulating miRNAs in acute myocardial infarction. Crit Rev Eukaryot Gene Expr. 2019;29(4).Doi:10.1615/CritRevEukaryotGeneExpr.2019028211.

4. Alonzo M, Delgado M, Cleetus C, Kumar SA, Thakur V, Chattopadhyay M, et al. Methods for histological characterization of cryo-induced myocardial infarction in a rat model. Acta Histochem. 2020;122(7):151624. Doi:10.1016/j.acthis.2020.151624.

5. van der Velden J, Asselbergs FW, Bakkers J, Batkai S, Bertrand L, Bezzina CR, et al. Animal models and animal-free innovations for cardiovascular research: current status and routes to be explored. Consensus document of the ESC Working Group on Myocardial Function and the ESC Working Group on Cellular Biology of the Heart. Cardiovasc Res. 2022;118(15):3016–51. Doi:10.1093/cvr/cvab370.

6. Tang Y ping, Liu Y, Fan Y jie, Zhao Y yang, Feng J qun, Liu Y. To develop a novel animal model of myocardial infarction: A research imperative. Anim Model Exp Med. 2018;1(1):36–9. Doi:10.1002/ame2.12010.

7. Liao J, Huang W, Liu G. Animal models of coronary heart disease. J Biomed Res. 2016;31(1):3.Doi:10.7555/JBR.30.20150051.

8. Kumar M, Kasala ER, Bodduluru LN, Dahiya V, Sharma D, Kumar V, et al. Animal models of myocardial infarction: Mainstay in clinical translation. Regul Toxicol Pharmacol. 2016;76:221–30. Doi:10.1016/j.yrtph.2016.03.005.

9 Nugroho J, Yuniarti WM, Wardhana A, Ghea C. Modification on acute myocardial infarction model through left anterior descending coronary artery ligation: An experimental study on rats (*Rattus norvegicus*) using readily available materials. Vet World. 2019;(9):1448. Doi: 10.14202/vetworld.2019.1448-1453.

10. Kolk MV V, Meyberg D, Deuse T, Tang-Quan KR, Robbins RC, Reichenspurner H, et al. LAD-ligation: a murine model of myocardial infarction. J Vis Exp. 2009;14(32):1438. Doi: 10.3791/1438.

11. De Villiers C, Riley PR. Mouse models of myocardial infarction: comparing permanent ligation and ischaemia-reperfusion. Dis Model Mech. 2020;13(11):dmm046565. Doi:10.1242/dmm.046565.

12. Martin TP, MacDonald EA, Elbassioni AAM, O'toole D, Zaeri AAI, Nicklin SA, et al. Preclinical models of myocardial infarction: from mechanism to translation. Br J Pharmacol. 2022;179(5):770–91. Doi:10.1111/bph.15595.

13. Duerr GD, Elhafi N, Bostani T, Ellinger J, Swieny L, Kolobara E, et al. Comparison of myocardial remodeling between cryo-infarction and reperfused infarction in mice. Biomed Res Int. 2011;2011(1):961298. Doi:10.1155/2011/961298.

14. Gao E, Koch WJ. A novel and efficient model of coronary artery ligation in the mouse. In: Wound Regeneration and Repair: Methods and Protocols. Springer; 2013. p. 299–311. Doi:10.1007/978-1-62703-505-7_17.

15. Lim GB. Clonal haematopoiesis induces a pro-inflammatory monocyte phenotype in HF. Nat Rev Cardiol. 2021;18(2):74.

Doi:10.1038/s41569-020-00481-5.

16. Bayat H, Swaney JS, Ander AN, Dalton N, Kennedy BP, Hammond HK, et al. Progressive heart failure after myocardial infarction in mice. Basic Res Cardiol. 2002;97:206–13. Doi:10.1007/s003950200013.

17. Reichert K, Colantuono B, McCormack I, Rodrigues F, Pavlov V, Abid MR. Murine left anterior descending (LAD) coronary artery ligation: an improved and simplified model for myocardial infarction. J Vis Exp. 2017;(122):55353. Doi:10.3791/55353.

18. Esmaeili R, Sadeghpour A, Darbandi-Azar A, Majidzadeh-A K, Vajhi A, Sadeghizadeh M. Echocardiographic assessment of myocardial infarction: comparison of a rat model in two strains. Iran J Vet Res. 2017;18(1):30.

19. Madadi F, Aghajani M, Dabbagh A, Fani K, Sehati F, Imani A. Effects of acute potassium chloride administration on ventricular dysrhythmias after myocardial infarction in a rat model of ischemia/reperfusion. J Tehran Univ Heart Cent. 2022;17(1):15. Doi:10.18502/jthc.v17i1.9320.

20. Vietta GG, Andrades ME, Dall'Alba R, Schneider SIR, Frick LM, Matte U, et al. Early use of cardiac troponin-I and echocardiography imaging for prediction of myocardial infarction size in Wistar rats. Life Sci. 2013;93(4):139–44. Doi:10.1016/j.lfs.2013.05.026.

21. Di Filippo C, Marfella R, Capodanno P, Ferraraccio F, Coppola L, Luongo M, et al. Acute oxygen-ozone administration to rats protects the heart from ischemia reperfusion infarct. Inflamm Res. 2008;57:445–9. Doi:10.1007/s00011-008-7237-0.

22. Naseroleslami M, Sharifi M, Rakhshan K, Mokhtari B, Aboutaleb N. Nesfatin-1 attenuates injury in a rat model of myocardial infarction by targeting autophagy, inflammation, and apoptosis. Arch Physiol Biochem. 2023;129(1):122–30. Doi:10.1080/13813455.2020.1802486.

23. Van Zuylen VL, Den Haan MC, Roelofs H, Fibbe WE, Schalij MJ, Atsma DE. Myocardial infarction models in NOD/Scid mice for cell therapy research: permanent ischemia vs ischemia-reperfusion. Springerplus. 2015;4(1):336. Doi:10.1186/s40064-015-1128-y.

24. Van den Bos EJ, Mees BME, De Waard MC, De Crom R, Duncker DJ. A novel model of cryoinjury-induced myocardial infarction in the mouse: a comparison with coronary artery ligation. Am J Physiol Circ Physiol. 2005;289(3):H1291--H1300. Doi:10.1152/ajpheart.00111.2005.

25. Dittrich A, Lauridsen H. Cryo-injury induced heart regeneration in the axolotl and echocardiography and unbiased quantitative histology to evaluate regenerative progression. J Vis Exp. 2021;171(171):e61966. Doi:10.3791/61966.

26. Farag A, Mandour AS, Hendawy H, Elhaieg A, Elfadadny A, Tanaka R. A review on experimental surgical models and anesthetic protocols of heart failure in rats. Front Vet Sci. 2023;10:1103229. Doi:10.3389/fvets.2023.110322.

27. Omoto ACM, do Carmo JM, Nelson B, Aitken N, Dai X, Moak S, et al. Central Nervous System Actions of Leptin Improve Cardiac Function After Ischemia-Reperfusion: Roles of Sympathetic Innervation and Sex Differences. J Am Heart Assoc. 2022;11(21):e027081. Doi:10.1161/JAHA.122.027081.

28. Wu Y, Yin X, Wijaya C, Huang MH, McConnell BK. Acute myocardial infarction in rats. J Vis Exp. 2011;(48):2464. Doi:10.3791/2464.

29. Ong SB, Kwek XY, Katwadi K, Hernandez-Resendiz S, Crespo-Avilan GE, Ismail NI, et al. Targeting mitochondrial fission using Mdivi-1 in a clinically relevant large animal model of acute myocardial infarction: a pilot study. Int J Mol Sci. 2019;20(16):3972. Doi:10.3390/ijms20163972.

30. Kalluri R, LeBleu VS. The biology, function, and biomedical applications of exosomes. Science (80-). 2020;367(6478):eaau6977. Doi:10.1126/science.aau6977.

31. Kerkhof PL, D'iaz-Navarro R, Heyndrickx GR, Handly N. A critical analysis of ejection fraction. Rev medica de Chile. 2022;150(2):232–40. Doi:10.4067/s0034-98872022000200232.

32. Lu Y, Liu JJ, Bi XY, Yu XJ, Kong SS, Qin FF, et al. Pyridostigmine ameliorates cardiac remodeling induced by myocardial infarction via inhibition of the transforming growth factor-β1/TGF-β1-Activated Kinase Pathway. J Cardiovasc Pharmacol. 2014;63(5):412–20. Doi:10.1097/FJC.0000000000000062.

33. Bayarsaikhan D, Bayarsaikhan G, Lee J, Lee B. A study on the protective effect of sRAGE-MSCs in a rodent reperfusion model of myocardial infarction. Int J Mol Sci. 2022;23(24):15630. Doi:10.3390/ijms232415630.

How to cite this article
Karimi A, Moghadam. Matin M, Haghighitalab A, Kazemi Mehrjerdi H, Rajabioun M, Aghasizadeh M, Bahrami AR. Cryo-infarction: a method of choice for the establishment of a rat model of myocardial infarction. Iran J Vet Sci Technol.2026; 18(2): 8-21.
DOI: https://doi.org/10.22067/ijvst.2025.93330.1533
URL: https://ijvst.um.ac.ir/article_48121.html